

1 **Inhibition of PDE4 by low doses of rolipram induces changes in lipid and protein components**
2 **of mice heart**

3
4
5
6

7 **Sevgi Türker-Kaya^{a*}, İpek Komsuoğlu Celikyurt^b, Umut Celikyurt^c, Aygül Kına^a**

8
9
10
11

12 ^aKocaeli University, Faculty of Arts and Sciences, Department of Biology, 41380, Kocaeli, TURKEY

13 ^bKocaeli University, Faculty of Medicine, Department of Pharmacology, 41380, Kocaeli, TURKEY

14 ^cKocaeli University, Faculty of Medicine, Department of Cardiology, 41380, Kocaeli, TURKEY

15
16
17

18 **Corresponding Author: S.Turker-Kaya**

19

20 Assist.Prof. Sevgi Türker-Kaya

21 Dept. of Biology, Kocaeli University,

22 Kocaeli, Turkey.

23 Tel: +090 262 303 28 08

24 Fax: +090 262 303 28 09

25 Email: sevgitrkr@gmail.com; sevgi.turker@kocaeli.edu.tr

1 **ABSTRACT**

2 Studies work on phosphodiesterase-4 (PDE4) inhibition in treatment of cardiovascular diseases. To
3 contribute this Fourier transform infrared spectroscopy offers promising approach due to its ability in
4 detection the changes in biomolecules. In the current study, we examined the effects of PDE4
5 inhibition by rolipram at 0.05 mg/kg and 0.1 mg/kg doses on content of lipids and proteins, and
6 fluidity, order and packing of membranes in naive mice heart. In treated groups, there was a
7 significant decrease in unsaturated, saturated lipids, cholesterol esters, fatty acids, phospholipids and
8 triacylglycerols obtained from CH_2 , $\text{C}=\text{O}$, olefinic= CH , and COO^- areas, and CH_2/lipid , $\text{C}=\text{O}/\text{lipid}$,
9 olefinic= CH/lipid , and $\text{COO}^-/\text{lipid}$ ratios. Additionally, olefinic= CH area and olefinic= CH/lipid ratio
10 may suggest decreased lipid peroxidation, confirmed by thiobarbituric acid assay. Also, a higher
11 degree of membrane order, slight increase in membrane fluidity and differences in membrane
12 packing were obtained. Amide I and II areas and RNA/protein ratios showed that variation in protein
13 content is not correlated with applied concentration. **Analysis of amide I mode predicted alterations**
14 **in secondary structures like an increase in random coils and decrease in alpha-helices.** Moreover, all
15 groups were successfully discriminated by cluster analysis. The corresponding results may help to
16 understand the potential effects of PDE4 inhibition by rolipram.

17

18

19

20

21

22

23

24

25 **Keywords:** Rolipram, heart, FTIR, lipid, protein, membrane order/packing/fluidity

1 **ABBREVIATIONS**

2

3	phosphodiesterase 4	PDE4
4	cyclic adenosine 3',5'-monophosphate	cAMP
5	Fourier Transform Infrared	FT-IR
6	phosphodiesterases	PDEs
7	infrared light	IR
8	dimethyl sulfoxide	DMSO
9	potassium bromide	KBr
10	buthylatedhydroxytoluene	BHT
11	malondialdehyde	MDA
12	trichloroacetic acid	TCA
13	thiobarbituric acid	TBA
14	standard deviation	SD
15	lipid peroxidation end products	LPEPs
16	reactive oxygen species	ROS

17

18

19

20

21

22

23

24

25

1 **1. INTRODUCTION**

2 Cyclic adenosine 3',5'-monophosphate (cAMP) is the main second messenger of β -adrenergic
3 receptor signalling inducing phosphorylation of L-type Ca^{+2} channels and ryanodine receptor to
4 increase the amount of intracellular Ca^{2+} necessary for heart contractility (Eschenhagen, 2013; Mika
5 et al., 2012). And, proper cardiac function relies on fine-tuning balance between the synthesis and
6 degradation of cAMP (Boullaran and Gales, 2015).

7 3',5'-cyclic nucleotide phosphodiesterases (PDEs) regulate the localization, duration, and
8 amplitude of the second messengers (Eschenhagen, 2013; Mika et al., 2012; Rao and Xi, 2009). Of
9 these, phosphodiesterase-4 (PDE4) enzymes **with subtypes of PDEA,B,C,D**, are crucial in shaping
10 global cAMP signals in cardiac myocytes in rodents (Verde et al., 1999) and in humans (Mika et al.,
11 2012; Molina et al., 2012). Thus, inhibition of PDE4s exhibits hemodynamic and inotropic properties
12 that may be valuable to clinical practice (Guglin and Kaufman, 2014; Molina et al., 2012; Goldhaber
13 and Hamilton, 2010). Related with this, numerous studies are focused on the mode action of PDE4
14 inhibitors with their side effects on heart. However, the overall picture of PDE4s inhibition with their
15 inhibitors is still uncertain and additional research is necessary for clinical applicability
16 (Eschenhagen, 2013; Mika et al., 2012; Molina et al., 2012; Rao and Xi, 2009). To contribute these
17 studies Fourier transform infrared (FT-IR) spectroscopy offers promising approach due to its ability
18 in detection of the changes on content, structure and dynamics of biomolecules in cells and tissues
19 (Turker-Kaya et al., 2016; Ozek et al., 2014; Derenne et al., 2012). It is a rapid technique that does
20 not require any staining nor complicated sample preparation (Turker et al., 2014a; Derenne et al.,
21 2012). Infrared (IR) spectrum of a biological sample represents the sum of various contributions from
22 lipids, proteins, carbohydrates, nucleic acids and all other chemical species (Turker et al., 2014a,b;
23 Ozek et al., 2014; Miller et al., 2013; Carmona et al., 2008). The intensities and/or areas provide
24 quantitative information, peak positions relate to physical states of molecules, and bandwidth gives
25 dynamical information (Turker-Kaya et al., 2016; Kumar et al., 2014; Turker et al., 2014a,b; Ozek et

1 al., 2014; Miller et al., 2013; Carmona et al., 2008; Severcan et al., 2005). As a result, it is possible to
2 monitor global effects of chemicals and conditions on all of the constituents in biological systems
3 (Turker-Kaya et al., 2016; Ozek et al., 2014; Gasper et al., 2009). By taking its advantages FT-IR
4 spectroscopy has been increasingly employed to investigate molecular alterations induced by drugs
5 and even disease' states, which is not easily detectable by morphological methods, in cells and tissues
6 (Turker-Kaya et al., 2016; Turker et al., 2014a,b; Bozkurt et al., 2012; Travo et al., 2012; Bellisola et
7 al., 2012; Cakmak et al., 2011; Berger et al., 2010; Akkas et al., 2007; Leskovjan et al., 2010;
8 Amharref et al., 2006).

9 There are different types of PDE4 inhibitors that show distinctive selectivity for PDE4
10 subtypes. For example, ibudilast has been shown to potently inhibit purified human PDE 4A, 4B, 4C
11 and 4D with IC50 values of 54, 65, 239 and 166 nM, respectively (Huang et al., 2006). Cilomilast is
12 ten-fold more selective for PDE4D compared to other PDE4 subtypes (Rennard et al., 2006). On the
13 other hand, roflumilast does not demonstrate any PDE4 subtype selectivity (Hatzelmann and Schudt
14 2001). Similarly, as being selective inhibitor of all isoenzymes of PDE4s rolipram, a well-
15 characterized PDE4 inhibitor, was developed as an effective antidepressant, and later tested for
16 treating asthma and chronic pulmonary disease (COPD) (McKenna et al., 2006). Although it was
17 hampered due to its gastrointestinal side effects, it has been still used in research investigating
18 potential use of PDE4 inhibition against several pathologies including cardiovascular diseases (Fu,
19 2014; Molina et al., 2012; Leroy et al., 2011; Kenk et al., 2010).

20 In the current study, we aimed to acquire a general point of view on the effects of PDE4
21 inhibition by rolipram at low concentrations (0.05 mg/kg and 1.0 mg/kg) on whole naive mice heart.
22 We have evaluated the variations of spectral parameters of control and rolipram treated groups as also
23 performed in previous studies (Turker-Kaya et al., 2016; Ozek et al., 2014; Bozkurt et al., 2012;
24 Cakmak et al., 2011). We have obtained the relative changes in lipid and proteins content, and
25 membrane lipid packing, membrane fluidity, and membrane order and lipid peroxidation, all of which

1 are very important parameters for proper function of heart. Moreover, by detailed analysis of Amide I
2 mode we also predicted the changes in protein secondary structures. We have successfully
3 discriminated control and treated groups depending on their spectra using cluster analysis (Turker et
4 al., 2014b; Severcan et al., 2010). To the best of our knowledge, such approach based on spectral
5 parameters resulted from PDE4 inhibition by rolipram action on naïve heart has been not reported,
6 previously.

7 2. MATERIAL AND METHOD

8 2.1 Animal care and drug treatment

9 Male inbred BALB/c mice (n=22) weighing 40 g (MAM TUBİTAK, Gebze, Kocaeli, Turkey), aged 7
10 weeks upon arrival the laboratory. The animals (4-5 per cage) were kept in the laboratory at $21 \pm$
11 1.5°C with 60% relative humidity under a 12 h light/dark cycle (light on at 8.00 p.m.) during 2 weeks
12 before experiments. Tap water and food pellets were available ad libitum. All procedures involving
13 animals were in compliance with the European Community Council Directive of 24 November 1986,
14 and ethical approval was granted by the Kocaeli University Ethics Committee (Number: AEK 9/4-
15 2010, Kocaeli, Turkey).

16 Rolipram were purchased from Sigma Chemical Company (Sigma, St.Louis, MO) and
17 dissolved in saline supplemented with small amounts of dimethyl sulfoxide (DMSO). The drug was
18 freshly prepared before intraperitoneally (i.p.) administration in a volume of 0.1 ml per 10 g body
19 weight. All animals were divided into three groups as control, 0.05 and 0.1 mg/kg. While control
20 group received vehicle, 0.05 and 0.1 mg/kg doses of rolipram were given to related treated groups for
21 each day during 15 days. At the end of the application procedure the animals were decapitated and
22 whole heart samples were dissected out and kept in -80°C till FTIR spectroscopic studies.

23 2.2 Sample Preparation for FT-IR Studies

24 To eliminate possible biological discrepancy among distinct heart regions where PDE4 activity is not
25 evenly distributed we prepared the samples from whole heart tissue. The whole heart samples were

1 dried in a Labconco freeze drier (Labconco FreeZone®, 6 liter Benchtop Freeze Dry System Model
2 77520) overnight in order to remove the water content. The samples were ground to obtain tissue
3 powder, which were later mixed with dried potassium bromide (KBr) at the ratio of 1/100. The
4 mixture was dried again in the freeze drier for 18 hours to remove all traces of remaining water. And
5 then, in order to obtain same thickness of each pellet same amount of sample was weighted and same
6 pressure $\sim 100\text{kg/cm}^2$ (1300psi) was applied to produce a thin KBr disk of all samples (Turker-Kaya
7 et al., 2016; Elibol-Can et al., 2011).

8 **2.3 FTIR spectroscopic analysis**

9 Infrared spectra were obtained using a Perkin-Elmer Spectrum One FTIR spectrometer (Perkin-Elmer
10 Inc., Norwalk, CT, USA) equipped with a MIR TGS detector. The spectra of samples were recorded
11 in the $4000\text{-}400\text{ cm}^{-1}$ region at room temperature. Each interferogram was collected with 100 scans at
12 4 cm^{-1} resolution. In order to remove the interference of water and carbondioxide effects on IR
13 spectra the spectrum of air and KBr transparent disk was recorded together as background and
14 subtracted automatically by using Spectrum One software (Perkin-Elmer).

15 Even though we performed special care to produce same thickness of each KBr pellet, to
16 minimize intra-sample variability which may be caused by variations in experimental conditions, we
17 scanned three independent pellets prepared by taking separate portions randomly from the same
18 sample. The average spectra of three replicates giving identical spectra represented one animal were
19 used in both detailed data analysis and statistical analysis as same approach performed in previous
20 studies (Akkas et al., 2007; Cakmak et al., 2011; Turker et al., 2014b; Ozek et al., 2014).

21 Spectrum One software were used to analysed spectral data by following earlier reports
22 (Turker-Kaya et al., 2016; Ozek et al., 2014; Elibol-Can et al., 2012). The band positions were
23 measured using the frequency corresponding to the center of 80% x height of the peak. The peak area
24 was calculated as related to a linear baseline between two baseline points which involve the
25 maximum peak height. The baseline point was identified according to start and end points of the

1 peak. Later, the corrected area which is the area between the spectrum and the marked baseline within
2 the marker bar limits was found the peak area value of the interested peak. The bandwidth values of
3 specific bands were calculated as the width at 0.80 x height of the signal in terms of cm^{-1} .

4 Again still considering possible interference due to detectable variability of sample thickness
5 area ratios of some specific IR modes were also evaluated to approximate content changes in
6 biomolecules since we did not apply any biochemical assay to measure content of biomolecules of
7 interest as performed previously (Turker-Kaya et al., 2016; Antoine et al., 2010). For the CH_2 /lipid,
8 $\text{C}=\text{O}$ /lipid, olefinic= CH /lipid, and COO^- /lipid ratios, the areas under the CH_2 asymmetric stretching
9 (2925 cm^{-1}), the $\text{C}=\text{O}$ stretching (1750 cm^{-1}), the olefinic= CH (3012 cm^{-1}), and the COO^- symmetric
10 (1390 cm^{-1}) modes were divided to the total saturated lipid (the sum of the area under the CH_2
11 asymmetric and symmetric stretching bands). For RNA/protein ratio, the area under C-N-C stretching
12 (998 cm^{-1}) were divided to the sum of the area under the amide I and II bands.

13 The same software was also used for smoothing, baseline correction and normalization
14 processes. The spectra were first smoothed with nineteen-point Savitsky-Golay smooth function to
15 remove the noise. And then, baseline correction was applied based on specific points. And,
16 normalization was performed with respect to specific bands. It should be worth noting that all these
17 procedures were performed only for visual representation of the differences among the groups. For
18 accurate evaluation of the spectral parameters the original average spectrum from each animal was
19 analyzed.

20 In order to predict the alterations in protein secondary structure elements, amide I mode was
21 further analyzed by OPUS 5.5 (Bruker Optic, GmbH). Since peak height/area of this mode is very
22 sensitive to changes of fullwidth at half height in second derivative spectra, concentration sensitive
23 changes in the components of this band were monitored by measuring intensity values of its sub
24 bands. The spectral comparisons of amide I band were carried out on vector normalized second
25 derivatives.

1 **2.4 Measurement of lipid peroxidation (TBARs assay)**

2 TBAR_S, well-adopted test, was performed to monitor lipid peroxidation (Turker et al., 2014a;
3 Severcan et al., 2005). The heart samples were homogenized by Teflon glass homogenizer in cold
4 0.02 M phosphate buffer (pH 7.4) at a concentration of 25 % (w/v). The homogenates were diluted to
5 5 % with the phosphate buffer containing 0.25 ml butylatedhydroxytoluene (BHT), which prevents
6 artificial increase of malonydialdehyde (MDA). Then, the homogenates were incubated for 60 min at
7 37 °C. After the incubation, 2 ml of trichloroacetic acid (TCA) solution (28 % w/v in 0.25 N HCl)
8 was added. The samples were centrifuged at low speed and 4 ml of supernatants were mixed with 1
9 ml of thiobarbituric acid (TBA) (1 % w/v in 0.25 N HCl). Subsequently, the samples were kept in
10 boiling water for 30 min to get chromophore development. The samples were cooled to room
11 temperature and the absorbance values were measured at 532 nm.

12 **2.5 Cluster Analysis**

13 Hierarchical cluster analysis was performed on first derivative spectra using the cluster analysis
14 module of OPUS 5.5 (Bruker Optic, GmbH). It was applied to distinguish between different spectra
15 from control and treated groups using a frequency range between 4000-800 cm⁻¹. As input data for
16 cluster analysis, spectral distances were calculated between pairs of spectra as Pearson's correlation
17 coefficients (Turker et al., 2014b; Severcan et al., 2010). Cluster analysis for separation of control and
18 rolipram treated heart tissues was based on the Euclidean distances. In all cases, Ward's algorithm
19 was used for hierarchical clustering.

20 **2.6 Statistical Analysis**

21 The results were expressed as 'mean ± standard deviation'. All data were analyzed statistically using
22 non-parametric ANOVA test. A 'p' value less than or equal to 0.05 was considered as statistically
23 significant. The degree of significance was denoted as less than or equal to p<0.05*.

24

25

3. RESULTS

Detailed spectral analysis revealed that there are prominent spectral differences in both rolipram treated groups compared to control ones. Depending on the spectral variations among groups in the region between 4000-800 cm^{-1} cluster analyses was performed to differentiate the groups. And, three distinct clusters were produced with a high accuracy (success rate 9/9 for 0.05 mg/kg, and 6/7 tissues for 0.1 mg/kg). The resultant dendogram is depicted in Figure 1.

In order to easily demonstrate the details of the spectral differences among the groups, the spectra were showed in two separated regions. Figure 2 and 3 show normalized infrared spectra of control, 0.05 mg/kg and 0.1 mg/kg dose of rolipram heart tissues in 3025-2800 cm^{-1} and 1940-800 cm^{-1} region, respectively. In Figure 2, the spectra were normalized with respect to the CH_2 asymmetric stretching band at 2925 cm^{-1} , and in Figure 3, the spectra were normalized with respect to the amide I band at 1645 cm^{-1} for visual demonstration of the spectral variations. The detailed band assignments based upon the literature were given in Table 1. Table 2 represents detailed analysis of spectral modes and results of TBAR's assay for each group.

The changes in the content of lipids have been relatively obtained by analysing the areas of the =CH olefinic (unsaturated lipids), the CH_2 asymmetric and the CH_2 symmetric (saturated lipids), the C=O (triacylglycerols, cholestereol esters and phospholipids) and the COO^- symmetric (fatty acids) as well as olefinic/lipid, CH_2 /lipid, C=O/lipid and COO^- /lipid ratios. As shown in Figure 2-3 and Table 2, in both treated groups all these areas and area ratios were significantly ($p < 0.05^*$) reduced.

As demonstrated in Table 2 and Figures 2-3, rolipram treatment at both two concentrations led to significant ($p < 0.05^*$) shiftings to lower values in the CH_2 asymmetric stretching (2925 cm^{-1}), the C=O (1750 cm^{-1}) and the PO_2^- symmetric (1080 cm^{-1}).

Alterations in fluidity of the cell membrane can be determined by probing the bandwidth values of the CH_2 asymmetric stretching mode (Ozek et al., 2014; Turker et al., 2014b; Lopez et al.,

1 2001). This value was slightly increased for 0.05 mg/kg and for 0.1 mg/kg rolipram as illustrated in
2 Figure 2 and Table 2.

3 The band areas of amide I and amide II modes are directly related with protein content in the
4 system (Turker et al., 2014a; Elibol-Can et al., 2011; Bozkurt et al., 2012) Figure 3 and Table 2
5 illustrate the areas of these modes significantly ($p<0.05^*$) increased for the group of 0.05 mg/kg
6 rolipram but significantly ($p<0.05^*$) decreased for 0.1 mg/kg rolipram group.

7 Amide I mode consists of many overlapping modes that represent different secondary
8 structure elements of proteins such as alpha-helices, beta-turns, turns and random coil (Turker et al.,
9 2014a; Turker-Kaya et al., 2016). Upon analysing of amide I band, the related peaks under amide I
10 were observed in second derivative spectra for control and treated groups (Figure 4). The band at
11 around 1682 cm^{-1} is associated with beta turns, the peak at 1652 cm^{-1} is due to alpha helix, the mode
12 located at 1643 cm^{-1} are assigned to random coil, beta sheet band appears at 1633 cm^{-1} coil (Turker et
13 al., 2014a; Turker-Kaya et al., 2016). The changes in the intensities of characteristics components of
14 amide I mode were given in Table 3. Compared to control for rolipram groups a decrement in alpha-
15 helix and beta-sheet ($p<0.05^*$) the intensity of beta sheet of amide I band was obtained. More
16 importantly, there is a statistically prominent increment in random coil for both rolipram groups
17 ($p<0.05^*$).

18 The band centered at 990 cm^{-1} is generally assigned to symmetric stretching mode of dianionic
19 phosphate monoester of cellular nucleic acids and ribose-phosphate main chain vibrations of the RNA
20 backbone (Ozek et al., 2014; Banyay et al., 2003; Chiriboga et al., 2000). There was a significant
21 ($p<0.05^*$) decrease in the area of this band and RNA/protein for both treated groups, indicating a
22 decrease in the nucleic acid, especially RNA content in heart tissue.

23

24

25

4. DISCUSSION

Whole heart tissue contains various components like cardiac myocytes, cardiac fibrocytes, endothelial cells and extracellular matrix. In such complexity FT-IR spectroscopy lacks providing information about each specific component. But, due to Conne' advantage it facilitates the vibrations of functional groups present in biomolecules to represent a variety of different modes appeared at distinct wavenumber values in an FT-IR spectrum. This enables separation of the peaks to be analysed even in weak absorption modes (Turker et al., 2014b; Leskovjan et al., 2010; Elibol-Can et al., 2011; Gasper et al., 2009).

In biological samples although FT-IR spectroscopy gives global information about biomolecules rather than specific ones, it is possible to detect saturated lipids, unsaturated lipids, cholesterol ester, triglycerides, proteins, nucleic acids and carbohydrates, as overall. Therefrom, the current study was conducted to obtain general perspective about the effects of PDE4 inhibition by rolipram on naïve whole mice heart by monitoring the variations in the frequencies, bandwidths and peak areas of the vibrational modes. The alterations in the spectral parameters between the control and treated groups were modest, but they were consistent and statistically significant with marginal standard deviations, as similarly reported (Turker–Kaya et al., 2016; Cakmak et al., 2011; Ozek et al., 2014). **Since there are significant changes among control and treated groups, cluster analysis successfully discriminated the spectra. In other words, this analysis revealed that low doses of rolipram administration give rise to important changes in FTIR spectra which can be effectively determined by its application as illustrated in Figure 1.**

As one of the disadvantages of FT-IR spectroscopy, it lacks providing quantitative information. But, according to Beer–Lambert law, the intensity and/or, more accurately, the area of absorption bands offer relative information for the content of corresponding functional groups within complex systems (Berger et al., 2010; Leskovjan et al., 2010). This has been previously confirmed by biochemical assays for lipid peroxidation products (LEPs) (Severcan et al., 2005; Leskovjan et al.,

1 2012; Turker et al., 2014a), proteins (Bozkurt et al., 2012) and lipids (Derenne et al., 2012). By
2 utilizing this, in the current study, we have evaluated areas and area ratios of lipid and protein modes
3 to approximate the changes in the content of these molecules without need of biochemical assays.

4 Lipid molecules are important regulators of cardiac function through their role in membrane
5 phospholipids, as signalling molecules and ligands for nuclear receptors, and as the predominant
6 oxidative substrate for cardiac mitochondria. As a general perspective action of PDE inhibitors
7 increase cAMP level, and thereby raise lipolysis in adipocytes (Chaves et al., 2011). This event may
8 cause deleterious consequences in some pathological conditions such as diabetes mellitus and obesity
9 (Arner et al., 2014; Perilli et al., 2013). Therefore, such inhibitors can be expected to produce some
10 effects on lipid metabolism which could be a potential risk factor for clinical adverse effect in heart.
11 Considering the administration of rolipram to stimulate lipolysis in brown fat tissue (Kraynik et al.,
12 2013) we have approximated the changes in content of lipid components like unsaturated, saturated
13 lipids, cholesterol esters, fatty acids, phospholipids and triacylglycerols. According to the obtained
14 results from the areas of the =CH olefinic, the CH₂ asymmetric, the CH₂ symmetric, the C=O, and
15 the COO⁻ symmetric stretching together with olefinic/lipid, CH₂/lipid, C=O/lipid and COO⁻/lipid
16 ratios, rolipram action has lowering effect on the content of heart lipids. Such decrement in fatty
17 acids, cholesterol esters and triacylglycerols might reveal utilization of these molecules for ATP
18 generation induced by PDE4 inhibition, which might be related with cAMP increasing effect on
19 mitochondrial function and cardiac contractility (Arner et al., 2014; Kajimoto et al., 1997). On the
20 other hand, as another types of lipids, phospholipids have not only pivotal impact on membrane
21 properties but also involve in specific signalling functions necessary for cells to respond to external
22 stimuli. For that reason, membrane phospholipid homeostasis is very important for heart. Related
23 with this, the found decrement in phospholipids together with saturated lipids in the current study has
24 importance for this and shows shortened chain lengths (Turker et al., 2014b). Moreover, such
25 outcome may be reflective of differences in phospholipid signalling that may contribute to the

1 progression of impaired heart function. In sum, it should be noting that the effects of rolipram on lipid
2 profile in the blood should be evaluated including levels of cholesterol like low and high density
3 lipoprotein. And, further studies are required to confirm the effects of rolipram on lipid content by
4 measuring lipoprotein lipase activity.

5 Heart tissue relies on oxidative pathway to utilize fuels, and has high content of mitochondria
6 where reactive oxygen species (ROS) are produced (Leary et al., 2003; Armstrong and Ianuzzo,
7 1977). These molecules readily attack lipids and lipid peroxidation occurs, and LEPs are released into
8 extra and intracellular site of cell (Turker et al., 2014a; Cakmak et al., 2011). Therefore, the detection
9 of LEPs may provide information about not only pathogenesis of any condition but also antioxidant
10 capacity of an agent in tissues including heart, also shown by reports in the literature (Ramana et al.,
11 2014; Battisti et al., 2008). In the current study, we have investigated whether PDE4 inhibition by
12 rolipram stimulates lipid peroxidation in heart, or not. Normally, when lipid peroxidation takes place,
13 an increase in olefinic mode area and olefinic/lipid ratio due to LEPs is observed as reported earlier
14 (Turker et al., 2014a). Moreover, when malondialdehyde (MDA), one of the LEPs, is produced, the
15 increment in the C=O mode and C=O/lipid ratio may be also observed (Cakmak et al., 2011). As
16 shown in Fig. 2-3 and Table 2, significant decreases in areas of the olefinic and C=O mode and
17 olefinic/lipid and C=O/lipid ratios may show low degree of lipid peroxidation, also confirmed by
18 decreased MDA levels (Table 2). Here, it should be pointed out that both used concentrations of
19 rolipram (0.05 and 0.1 mg/kg) decreased the content of MDA to approximately the same level. It is
20 very well known that the production of MDA occurs by utilization of unsaturated lipids. As we found
21 that 0.1 mg/kg rolipram has more decreasing effect on the content of unsaturated lipids as obtained
22 from reduced area of olefinic mode at 3012 cm^{-1} . This may result in less MDA level produced than
23 expected. The decrement in LEPs might be resulted from intracellular cAMP level, which can
24 suppress the burst of ROS generation (Azadbar et al., 2009). Hence, this finding which showed

1 decreasing effect of rolipram action on lipid peroxidation level in heart also extends the previous
2 reports performed in different tissues (Jindal et al., 2015; Rezvanfar et al., 2010).

3 Cardiac action potential is critically dependent on membrane compartments which are proteins
4 and lipids. For that reason, the determination of PDE4 inhibition-stimulated changes on membranes
5 has great importance in understanding the effects of this phenomenon on the proper function of heart.
6 So, we have focused on membrane structure, fully mediated through physical properties of fatty acids,
7 polar head groups of lipids, as well as lipid order, lipid fluidity and content of membrane
8 components. However, it should be also mentioning that, our sample contains all membranous
9 structures within heart tissue such as sarcolemma, plasma membrane, sarcoplasmic reticulum, and
10 nuclear membrane. Since our preparation contains all membrane compartments, membrane related
11 parameters might reflect the differences in all membrane systems in heart from control and rolipram
12 groups from a general perspective.

13 The found decline in the content of phospholipids which also show altered lipid composition
14 further affects the organization and packing of lipids (Derek et al., 1990; Akkas et al., 2007; Turker et
15 al., 2014b). In order to get information about lipid packing parameter we have analyzed the frequency
16 changes of the CH₂ asymmetric, the C=O and the PO₂⁻ symmetric, which reveal the physical state of
17 fatty acyl chains and head groups of membrane phospholipids. The CH₂ stretching vibrations depend
18 on the degree of conformational disorder; hence they can be used to monitor trans/gauche
19 isomerization in the system (Amharref et al., 2006; Ozek et al., 2014; Turker et al., 2014b). The
20 significant shifting to lower values in the CH₂ asymmetric mode may represent an increment in the
21 order of the system, which presents an increase in the number of trans conformers resulting in more
22 rigid membranes (Turker-Kaya et al., 2016; Elibol-Can et al., 2011; Akkas et al., 2007). Additionally,
23 significantly lowered wavenumber values of the C=O and the PO₂⁻ symmetric bands may imply an
24 increase in the hydration state of the glycerol backbone near the hydrophilic part and polar head
25 group of the membrane lipids. The hydrogen bonding might be between water molecules and the

1 oxygen molecules of both carbonyl and phosphate groups of phospholipids (Turker et al., 2014b;
2 Carmona et al., 2008; Akkas et al., 2007). The variations in physical state of membrane phospholipids
3 may further affect their interaction with hydrophobic and hydrophilic residues of membrane proteins
4 (Turker et al., 2014b). Furthermore, such outcome may have an effect on the functions of glycolipids
5 and glycoproteins which may operate as cell receptors and be responsible for cell signalling
6 (Saberwall and Nagaraj, 1994). All of these structural changes in membranes may alter the activity of
7 membrane proteins.

8 Lipid organization and composition predominantly determine membrane fluidity, which is
9 important for a number of activities including membrane transport, enzyme activity, chemical
10 secretion, and receptor binding and stimulation (Antoine et al., 2010; Derek et al., 1990). The found
11 slight increment in the bandwidth value of CH₂ asymmetric stretching mode indicates minor effect of
12 PDE4 inhibition by rolipram on fluidity of heart tissue membranes (Turker et al., 2014b; Elibol-Can
13 et al., 2011; Akkas et al., 2007). This might be resulted from a decrease in low content of cholesterol
14 obtained from lower area of C=O and C=O/lipid ratio.

15 An interesting finding is that applied concentrations of rolipram are not correlated with the
16 changes in protein content obtained from a significant increase for 0.05 mg/kg but decrease for 0.1
17 mg/kg rolipram in amide I and amide II mode areas, respectively. This may not be contributed to
18 synthesis of some proteins since there was a significant decrease in RNA content with increasing
19 concentration (Bozkurt et al., 2012; Banyay et al., 2003; Chiriboga et al., 2000). **On the other hand, it**
20 **has been reported in the literature that increasing concentration rolipram leads to reduction in muscle**
21 **protein degradation (Lira et al., 2011). An increase in amide I band area for 0.05 mg/kg might be**
22 **related with this. However, amide I results indicated that besides reducing proteolysis rolipram has**
23 **also effects on protein profile of whole heart that is non-linearly related with doses.** In order to bring
24 conclusion about rolipram action effects on cardiac proteins content the more extensive experimental
25 design studying larger range of concentrations with even isolated proteins would be beneficial.

1 Since amide I and amide II profiles also depend on the protein structural composition, the
2 changes in areas and amide I/amide II ratio may suggest that there are some alterations in the
3 structures of proteins (Turker et al., 2014b). Moreover, in recent medical research it has been shown
4 that, compared with the normal tissue, the diseased tissue shows a change in protein secondary
5 structure and ratio of amide I to amide II (Szczerbowska-Boruchowska et al., 2007). In order to better
6 estimate the alterations in protein structure amide I mode was further analysed as performed in earlier
7 studies (Turker-Kaya et al., 2016; Turker et al., 2014b; Akkas et al., 2007). The results of this study
8 showing significant increase in random coils but decrease in alpha helix and beta sheet structures
9 ($p < 0.05^*$) might reveal structural change in proteins for rolipram groups. Such changes give
10 information data about protein functions since there is strict relation with their functions and
11 structures. Taking this into consideration, our findings, particularly increase in random coils, reveal
12 denaturation leading to dysfunction of proteins for rolipram groups (Turker-Kaya et al., 2016; Turker
13 et al., 2014b; Akkas et al., 2007). This finding is obviously valuable data since heart muscle
14 contraction is brought about by the interaction of multiple proteins in subcellular structures such as
15 actin, myosin, tropomyosin and troponins. Additionally, again, our preparation contains all membrane
16 compartments, these parameters may be also attributed to the differences in all membrane proteins in
17 heart from control and rolipram groups from a general perspective. For example, a decrease in alpha-
18 helices and beta-sheet structures might suggest that there are changes in membrane lipids between
19 these molecules. This further means that membrane spanning domains of these proteins are then
20 conformationally altered to stabilize membrane curvature (Turker et al., 2014b). All these changes
21 may probably have importance for the regulation of protein functions in heart during PDE4 inhibition.
22 As suggested by Kitsis et al. (1996) such abnormalities in these molecules, major structural and
23 functional components of heart tissue, have been postulated to be the cause of contractile dysfunction.
24 These include further cell death and cellular dysfunctions involving contractile proteins, sarcolemma
25 (including associated receptors and channels), sarcoplasmic reticulum and other components of the

1 excitation-contraction coupling apparatus, mitochondria and associated anabolic proteins and various
2 signal transduction. Similarly, it has been reported that unfolded protein response system designed to
3 shut down protein synthesis regulates cardiac sodium current in systolic human heart failure (Gao et
4 al., 2012).

5 5. CONCLUSION

6 The present study investigated the effects of PDE4 inhibition by rolipram with low two different
7 doses (0.05 and 0.1 mg/kg) in mice heart by FT-IR spectroscopy at molecular level. Detail spectral
8 analysis revealed that rolipram action caused significant changes in the macromolecular content,
9 structure and function in heart tissue. The data indicated differences in membrane packing and a
10 significant decrease in lipid, RNA content, lipid peroxidation but an increase in membrane fluidity
11 and membrane order. Additionally, the change in protein content was found not to be in line with
12 applied concentrations of rolipram. An altered structural profile for proteins was predicted with an
13 increase in random coil whereas a decrease in beta sheet and alpha-helices in both treatment groups.

14 Depending on these spectral variations control and treated groups could be successfully discriminated
15 by cluster analysis. All these monitored parameters are very important for structure of heart tissue and
16 any change in any of these may further affect its proper functions. For example, alterations in lipids
17 can be observed in myocardial infarction, cardiac arrhythmia and heart failure (Nordestgaard,
18 2014; Bui, 2011; Moe and Wong, 2010; Mandel, 1995). Furthermore, as reported that formation of
19 free radicals and decrease in unsaturated lipids have prominent roles in cardiovascular disease,
20 particularly, atherosclerosis and the associated adverse complications (Thomas and Hazen, 2010;
21 Smyth et al., 2009;). Moreover, modification in membrane structure in the heart muscle can affect
22 various functions of the membranes by affecting membrane-bound enzymes and receptors directly or
23 indirectly by change in fluidity or permeability of the membranes (Holman, 1981; Gudbjarnason and
24 Oskarsdottir, 1977;). Together with such membrane related alterations changes in protein structures
25 may also cause cardiovascular diseases such as contractile dysfunctions, cardiac amyloidosis,

1 cardiomyopathy and arrhythmia (Moe and Wong, 2010; Mandel, 1995). For that reason, the findings
2 of the current study can provide a basis for the research on PDE4 inhibition by low doses rolipram, a
3 well-characterized PDE4 inhibitor, and for development of new PDE4 inhibitors. However, in order
4 to clarify the effects of PDE4 inhibition on heart tissue additional studies including comparison of
5 different PDE4 inhibitors on different animal models of heart failure and arrhythmias should be
6 performed.

7
8
9
10
11
12
13
14
15
16
17
18
19
20
21
22
23
24
25

1 **REFERENCES**

- 2 Akkas S. B., Inci S., Zorlu F., Severcan F. (2007): Melatonin affects the order, dynamics and
3 hydration of brain membrane lipids. *J. Mol. Struct.* 834–836, 207–215.
- 4 Amharref N., Beljebbar A., Dukic S., Venteo L., Schneider L., Pluot M., Vistelle R. (2006): Brain
5 tissue characterisation by infrared imaging in a rat glioma model. *Biochim. Biophys. Acta* 1758, 892–
6 899.
- 7 Antoine K. M., Mortazavi S., Miller A. D., Miller L.M. (2010): Chemical differences are observed in
8 childrens' versus adults' fingerprints as a function of time. *J. Forensic. Sci.* 55, 513–518.
- 9 Armstrong R. B., Ianuzzo C.D. (1977): Compensatory hypertrophy of skeletal muscle fibers in
10 streptozotocin-diabetic rats. *Cell Tiss. Res.* 181, 255-266.
- 11 Arner P., Langin D. (2014): Lipolysis in lipid turnover, cancer cachexia, and obesity-induced insulin
12 resistance. *Trends Endocrinol. Metab.* 25, 255–62.
- 13 Azadbar M., Ranjbar A., Hosseini-Tabatabaei A., Golestani A., Baeeri M., Sharifzadeh M. (2009):
14 Interaction of phosphodiesterase 5 inhibitor with malathion on rat brain mitochondrial-bound
15 hexokinase activity. *Pestic. Biochem. Physiol.* 95, 121–125.
- 16 Banyay M., Sarkar M., (2003): A library of IR bands of nucleic acids in solution. *Biophys. Chem.*
17 104, 477–88.
- 18 Battisti V., Maders L. D., Bagatini M. D., Santos K. F. (2008): Measurement of oxidative stress and
19 antioxidant status in acute lymphoblastic leukemia patients. *Clin. Biochem.* 41, 511-518.
- 20 Bellisola G., Sorio C. (2012): Infrared spectroscopy and microscopy in cancer research and diagnosis.
21 *Am. J. Cancer Res.* 2, 1-21.
- 22 Berger G., Gasper R., Lamoral-Theys D., Wellner A., Gelbcke R., Gust J. (2010): Fourier Transform
23 Infrared (FTIR) spectroscopy to monitor the cellular impact of newly synthesized platinum
24 derivatives. *Int. J. Oncol.* 37, 679–686.

1 Boularan C., Gales C. (2015): Cardiac cAMP:production, hydrolysis, modulation and detection.
2 Front. Pharmacol. 6, 203-207.

3 Bozkurt O., Bayari S. H., Severcan M., Krafft C., Popp J., Severcan F. (2012): Structural alterations
4 in rat liver proteins due to streptozotocin-induced diabetes and the recovery effect of selenium:
5 Fourier transform infrared microspectroscopy and neural network study. 17, 076023.

6 Bui A. L., Horwich T. B., Fonarow G.C. (2011): Epidemiology and risk profile of heart failure.
7 Nature Rev. Cardio. 8, 30–41.

8 Cakmak G., Zorlu F., Severcan M., Severcan F. (2011): Screening of protective effect of amifostine
9 on radiation-induced structural and functional variations in rat liver microsomal membranes by FT-IR
10 spectroscopy. Anal. Chem. 83, 2438–2444.

11 Carmona P., Rodríguez-Casado A., Alvarez I. (2008): FTIR microspectroscopic analysis of the
12 effects of certain drugs on oxidative stress and brain protein structure. Biopol. 89, 548-54.

13 Chaves V. E., Frasson D., Kawashita N.H. (2011): Several agents and pathways regulate lipolysis in
14 adipocytes. Biochimie. 93, 1631–40.

15 Chiriboga L., Yee H., Diem M. (2000): Infrared spectroscopy of human cells and tissues. Part VI: A
16 comparative study of histopathology and infrared microspectroscopy of normal, cirrhotic, and
17 cancerous liver tissue. Appl. Spectrosc. 54, 1-8.

18 Curatolo W. (1987): Glycolipid function. Biochim. Biophys. Acta 906, 137–160.

19 Derek M. (1990): Lipid-protein interactions in membranes. FEBS 6, 61-66.

20 Derenne A., Hemelryck V., Lamoral-Theys D., Kiss R., Goormaghtigh E. (2012): FTIR spectroscopy:
21 a new valuable tool to classify the effects of polyphenolic compounds on cancer cells. Biochim.
22 Biophys. Acta 1832, 46-56.

23 Elibol-Can B., Jakubowska-Dogru E., Severcan M., Severcan F. (2011): The effects of short-term
24 chronic ethanol intoxication and ethanol withdrawal on the molecular composition of the rat
25 hippocampus by FT-IR spectroscopy. Alcohol Clin. Exp. Res. 35, 2050-2062.

1 Eschenhagen T. (2013): PDE4 in the human heart - major player or little helper? *Br. J. Pharmacol.*
2 169, 524-527.

3 Fu Q. (2014): A Long Lasting β 1 Adrenergic Receptor Stimulation of cAMP/Protein Kinase A (PKA)
4 Signal in Cardiac Myocytes. *J. Biol. Chem.* 10, 14771-14781.

5 Gao G., Xie A., Zhang J., Herman M., Liu M. (2013): Unfolded protein response regulates cardiac
6 sodium current in systolic human heart failure. *Circ: Arrhythm. Electrophysiol.* 6, 1018.

7 Gasper R., Dewelle J., Kiss R., Mijatovic T., Goormaghtigh E. (2009): IR spectroscopy as a new tool
8 for evidencing antitumor drug signatures. *Biochim. Biophys. Acta* 1788, 1263-70.

9 Goldhaber J., Hamilton M. (2010): The role of inotropic agents in the treatment of heart failure.
10 *Circul.* 121, 1655-1660.

11 Gudbjarnason S., Oskarsdottir. (1977): Modification of fatty acid composition of rat heart lipids by
12 feeding cod liver oil. *Biochim. Biophys. Acta.* 487, 10-15.

13 Guglin M., Kaufman M. (2014): Inotropes do not increase mortality in advanced heart failure. *Int. J.*
14 *Gen. Med.* 7, 237-251.

15 Harvey P. A., Leinwand L. A. (2011): Cellular mechanisms of cardiomyopathy. *J Cell. Biol.* 194,
16 355–365.

17

18 Hatzelmann A., Schudt C. (2001): Anti-inflammatory and immunomodulatory potential of the novel
19 PDE4 inhibitor roflumilast in vitro. *J Pharmacol. Exp. Ther.* 1, 267–279.

20 Holman R. T. (1981): Nutritional and metabolic interrelationships between fatty acids. *Fed. Proc.* 23,
21 1062-1067.

22 Huang Z., Liu S., Zhang L., (2006): Preferential inhibition of human phosphodiesterase 4 by
23 ibudilast. *Life Sci.* 78, 2663–2668.

24 Jindal A., Manesh R., Bhatt S. (2015) Type 4 phosphodiesterase enzyme inhibitor, rolipram rescues
25 behavioral deficits in olfactory bulbectomy models of depression: Involvement of hypothalamic-

1 pituitary-adrenal axis, cAMP signaling aspects and antioxidant defense system. *Pharmacol. Biochem.*
2 *Behav.* 132, 20-32.

3 Kajimoto K., Hagiwara N., Kasanuki H., Hosoda S. (1997) Contribution of phosphodiesterase
4 isozymes to the regulation of the L-type calcium current in human cardiac myocytes. *Br. J.*
5 *Pharmacol.* 121, 1549–56.

6 Kenk M., Thackeray J.T., Chow B.J. (2010). Alterations of pre- and postsynaptic noradrenergic
7 signaling in a rat model of adriamycin-induced cardiotoxicity. *J. Nucl. Cardiol.* 17, 254-263.

8 Kitsis M.D., Scheuer J. (1996): Functional significance of alterations in cardiac contractile protein
9 isoforms. *Clin. Cardiol.* 19, 9-18.

10 Kraynik S.M., Miyaoka R.S., Beavo J.A. (2013): PDE3 and PDE4 Isozyme-selective inhibitors are
11 both required for synergistic activation of brown adipose tissue. *Mol. Pharmacol.* 83, 1155-1165.

12 Kumar S., Reena S., Chaudhary S., (2014): Vibrational studies of different human body disorders
13 using FTIR spectroscopy. *Open J. App. Sci.* 4, 103-129.

14 Leary S.C., Lyons C.N., Rosenberger A.G., Ballantyne J.S., Stillman J., Moyes C.D. (2003): Fiber-
15 type differences in muscle mitochondrial profiles. *Am. J. Physiol. Regulatory Integrative Comp.*
16 *Physiol.* 285, 817-826.

17 Leroy J., Fischmeister R., Vandecasteele G. (2011) Phosphodiesterase 4B in the cardiac L-type Ca²⁺
18 channel complex regulates Ca²⁺ current and protects against ventricular arrhythmias in mice. *J. Clin.*
19 *Invest.* 121, 2651-2661.

20 Leskovjan A., Kretlow A., Miller L. (2010): Fourier transform infrared imaging shows reduced
21 unsaturated lipid content in the hippocampus of a mouse model of Alzheimer's disease. *Anal Chem*
22 82, 2711-2716.

23 Lira E.C., Goncalves D.A., Parrerias-E-Silva L.T., Zanon N.M., Kettelhut I.C., Navegantes L.C.,
24 (2011): Phosphodiesterase-4 inhibition reduces proteolysis and atrogenes expression in rat skeletal
25 muscles. *Muscle Nerve.* 44, 371-381.

1 Lopez G., Martinez R., Gallego J., Tarancon M.J., Carmona P., Fraile M.V. (2001): Dietary fats
2 affect rat plasma lipoprotein secondary structure as assessed by fourier transform infrared
3 spectroscopy. *J. Nutr.* 131, 1898–1902.

4 Mandel, William J., ed. (1995). *Cardiac Arrhythmias: Their Mechanisms, Diagnosis, and*
5 *Management* (3 ed.). Lippincott Williams & Wilkins.

6 McKenna, J.M., Muller, G.W., *Medicinal Chemistry of PDE4 Inhibitors*. In: Beavo J, editors. *Cyclic*
7 *Nucleotide Phosphodiesterases in Health and Disease*, New York: CRC Pres; 2006.

8 McIntyre T. M., Hazen S. L. (2010): Lipid oxidation and cardiovascular disease: Introduction to a
9 review series circulation research. *Cir. Res.* 107, 1167-1169.

10 Mika D., Leroy J., Vandecasteele G., Fischmeister R. (2012): PDEs create local domains of cAMP
11 signaling. *J. Mol. Cell. Cardiol.* 52, 323-9.

12 Miller L. M., Bourassa M. W., Smith R. J. (2013): FTIR spectroscopic imaging of protein aggregation
13 in living cells. *BBA-Biomem.* 1828, 2339-2346.

14 Moe K. T., Wong P. (2010): Current trends in diagnostic biomarkers of acute coronary syndrome.
15 *Ann. Acad. Med. Singap.* 39, 210–215.

16 Molina C.E., Leroy J., Richter W., Xie M., Scheitrum C. (2012): Cyclic adenosine monophosphate
17 phosphodiesterase type 4 protects against atrial arrhythmias. *J. Am. Coll. Cardiol.* 59, 2182-90.

18 Nordestgaard B. (2014): Triglycerides and cardiovascular disease. *Lancet.* 384, 626-635.

19 Ozek N.S., Bal B., Sara Y., Onur R., Severcan F. (2014): Structural and functional characterization of
20 simvastatin-induced myotoxicity in different skeletal muscles. *BBA-General Subj.* 406, 406-415.

21 Perilli G., Saraceni C., Daniels M.N., Ahmad A. (2013): Diabetic ketoacidosis: a review and update.
22 *Curr. Emerg. Hosp. Med. Rep.* 1, 10–7.

23 Ramana K., Srivastava S., Singhal S. (2014): Lipid peroxidation products in human health and
24 disease. *Oxidative Medicine and Cellular Longevity* 162, 1-3.

1 Rao J.Y., Xi L. (2009): Pivotal effects of phosphodiesterase inhibitors on myocyte contractility and
2 viability in normal and ischemic hearts. *Acta Pharmacol. Sin.* 30, 1-24.

3 Rennard S.I., Schachter N., Streck M., (2006): Cilomilast for COPD: results of a 6-month, placebo-
4 controlled study of a potent, selective inhibitor of phosphodiesterase 4. *Chest.* 1, 56–66.

5 Rezvanfar M. A., Ranjbar A. (2010): Biochemical evidence on positive effects of rolipram a
6 phosphodiesterase-4 inhibitor in malathion-induced toxic stress in rat blood and brain mitochondria.
7 *Pestic Biochem. Physiol.* 98, 135–43.

8 Saberwal G., Nagaraj R. (1994): Cell-lytic and antibacterial peptides that act by perturbing the barrier
9 function of membranes: facets of their conformational features, structure-function correlations and
10 membrane-perturbing abilities. *Biochim. Biophys. Acta – Rev. on Biomemb.* 1197, 109-131.

11 Szczerbowska-Boruchowska M., Dumas P., Kastyak M., Chwiej J. (2007): Biomolecular
12 investigation of human substantia nigra in Parkinson's disease by synchrotron radiation Fourier
13 transform infrared microspectroscopy. *Archiv. Biochem. Biophys.* 459, 241–248.

14 Severcan F., Bozkurt O., Gurbanov R., Gorgulu G. (2010): FT-IR spectroscopy in diagnosis of
15 diabetes in rat animal model. *J. Biophoton.* 3, 621–626.

16 Severcan F., Gorgulu G., Turker S., Gorgulu S.T., Guray T. (2005): Rapid monitoring of diabetes-
17 induced lipid peroxidation by Fourier transform infrared spectroscopy: evidence from rat liver
18 microsomal membranes. *Anal. Biochem.* 39, 36–40.

19 Smyth E. M., Grosser T., Wang M., Yu Y., FitzGerald G. A. (2009): Prostanoids in health and
20 disease. *J Lipid Res.* 50, Suppl:S423–428.

21 Travo A., Desplat V., Barron E., Poychicot-Coustau J., Guillon, G. Déléris I. (2012): Basis of a FTIR
22 spectroscopy methodology for automated evaluation of Akt kinase inhibitor on leukemic cell lines
23 used as model. *Anal. Bioanal. Chem.* 404, 1733–1743.

- 1 Turker S., Ilbay, G., Severcan M., Severcan F. (2014a): Investigation of compositional, structural, and
2 dynamical changes of pentylenetetrazol-induced seizures on a rat brain by FT-IR spectroscopy. Anal
3 Chem 86, 1365-1403.
- 4 Turker S., Ilbay, G., Severcan M., Severcan F. (2014b): Epileptic seizures induce structural and
5 functional alterations on brain tissue membrane. BBA-Biomem. 1838, 3088-3096.
- 6 Turker-Kaya S., Mutlu O., Çelikyurt I.K., Akar F., Ulak G. (2016): Tianeptine, olanzapine and
7 fluoxetine show similar restoring effects on stress induced molecular changes in mice brain: An FT-
8 IR study Spectrochi. Acta Part A: Mol. Biomol. Spectr. 161, 178–185.
- 9 Verde I., Vandecasteele G., Lezoualc'h F., Fischmeister R. (1999): Characterization of the cyclic
10 nucleotide phosphodiesterase subtypes involved in the regulation of the L-type Ca²⁺ current in rat
11 ventricular myocytes. Br. J. Pharmacol. 127, 65-74.

ACKNOWLEDGEMENT

This study is supported by Scientific Research Foundation (BAP) Kocaeli University Turkey (AEK-9/4-2010).

CONFLICT OF INTEREST

We wish to confirm that there are no known conflicts of interest associated with this publication and there has been no significant financial support for this work that could have influenced its outcome.

FIGURE LEGENDS

Figure 1. Hierarchical analysis of control, 0.05 mg/kg rolipram, and 0.1 mg/kg rolipram groups for 4000-800 cm^{-1} spectral region.

Figure 2. Representative FT-IR spectra of control (black line), 0.05 mg/kg rolipram (blue line), and 0.1 mg/kg rolipram (red line) groups in the region between 3050-2830 cm^{-1} . The spectra were normalized with respect to the CH_2 asymmetric stretching at 2925 cm^{-1} .

Figure 3. Representative FT-IR spectra of control (black line), 0.05 mg/kg rolipram (blue line), and 0.1 mg/kg rolipram (red line) groups in the region between 1940-840 cm^{-1} . The spectra were normalized with respect to the Amide I at 1645 cm^{-1} .

Figure 3. Representative FT-IR spectra of control (black line), 0.05 mg/kg rolipram (blue line), and 0.1 mg/kg rolipram (red line) groups in the region between 1940-840 cm^{-1} . The spectra were normalized with respect to the Amide I at 1645 cm^{-1} .

Figure 4. Representative the second derivative spectra of amide I band for control (black line), 0.05 mg/kg rolipram (blue line), and 0.1 mg/kg rolipram (red line) groups in the region between 1700-1600 cm^{-1} . Vector normalization was done in the 1700-1600 cm^{-1} region. Absorption maxima appear as minima in the second derivatives.

TABLES

Table 1. General band assignment of heart tissue

Frequency (cm ⁻¹)	Definition of the Spectral Assignments
3012	Olefinic =CH stretching: unsaturated lipids
2925	CH ₂ asymmetric stretching: mainly lipids with little contribution from proteins, carbohydrates and nucleic acids
2852	CH ₂ symmetric stretching: mainly lipid with the little contribution from proteins, carbohydrates and nucleic acids
1750	Saturated ester C=O stretch: phospholipids, cholesterol esters, triglycerides
1645	Amide I (protein C=O stretch): proteins
1547	Amide II (C=N and N-H stretching): proteins
1450	COO ⁻ symmetric stretching: fatty acids
1080	PO ₂ ⁻ symmetric stretching: phospholipids and nucleic acids
976	C ⁺ -N-C stretching: nucleic acids, ribose phosphate main chain vibrations of RNA

Table 2. The frequency, band area and area ratio values of FTIR bands and MDA levels for control, 0.05 mg/kg and 0.1 mg/kg of rolipram for heart tissue. The values are the mean \pm standart deviation for each sample. The degree of significance was denoted as (p<0.05*).

	Control	0.05 mg/kg	0.1 mg/kg
Frequency			
CH ₂ asym	2924.09 \pm 0.07	2922.14 \pm 0.28*	2921.88 \pm 0.44*
C=O	1753.10 \pm 0.89	1750.62 \pm 1.30*	1750.09 \pm 0.91*
PO ₂ sym	1080.92 \pm 0.58	1077.99 \pm 1.63*	1076.81 \pm 1.12*
Band Areas			
olefinic	1.78 \pm 0.11	1.09 \pm 0.07*	0.34 \pm 0.09**
CH ₂ asym	13.59 \pm 0.76	12.68 \pm 0.14*	11.27 \pm 0.68*
C=O	2.91 \pm 0.03	1.07 \pm 0.08*	0.90 \pm 0.05*
amide I	25.46 \pm 0.78	28.51 \pm 0.49*	20.09 \pm 1.36*
amide II	12.27 \pm 1.43	14.70 \pm 1.41*	10.05 \pm 0.83*
COO ⁻	3.90 \pm 0.06	3.11 \pm 0.17*	3.22 \pm 0.34*
RNA	4.78 \pm 0.67	3.87 \pm 0.39*	3.79 \pm 0.86*
Band Area Ratio Values			
olefinic/lipid	0.08 \pm 0.002	0.05 \pm 0.009*	0.02 \pm 0.004*
CH ₂ /lipid	0.61 \pm 0.009	0.58 \pm 0.007*	0.57 \pm 0.006*
C=O/lipid	0.13 \pm 0.008	0.05 \pm 0.006*	0.04 \pm 0.001*
COO ⁻ /lipid	0.17 \pm 0.002	0.14 \pm 0.002*	0.15 \pm 0.003*
RNA/protein	0.12 \pm 0.007	0.09 \pm 0.008*	0.10 \pm 0.005*
Bandwidth			
CH ₂ asym	8.44 \pm 0.13	8.65 \pm 0.16	8.87 \pm 0.95
TBARs assay			
MDA (nmol/g)	39.44 \pm 2.27	30.05 \pm 1.88*	31.54 \pm 2.90*

Table 3. The changes in value of protein secondary structure estimation by second derivative for control, 0.05 mg/kg and 0.1 mg/kg of rolipram for heart tissue. The values are the mean \pm standart deviation for each sample. The degree of significance was denoted as (p<0.05*).

	Control	0.05 mg/kg rol.	0.1 mg/kg rol.
1-Beta turn	-0.0022 \pm 0.0004	- 0.0019 \pm 0.0002*	- 0.0018 \pm 0.0003*
2-Alpha helix	- 0.0049 \pm 0.0002	- 0.0045 \pm 0.0006*	- 0.0043 \pm 0.0007*
3-Random coil	- 0.0021 \pm 0.0005	- 0.0024 \pm 0.0009*	- 0.0025 \pm 0.0001*
4-Beta sheet	- 0.0036 \pm 0.0007	-0.0026 \pm 0.0004	- 0.0023 \pm 0.0006*

Heterogeneity

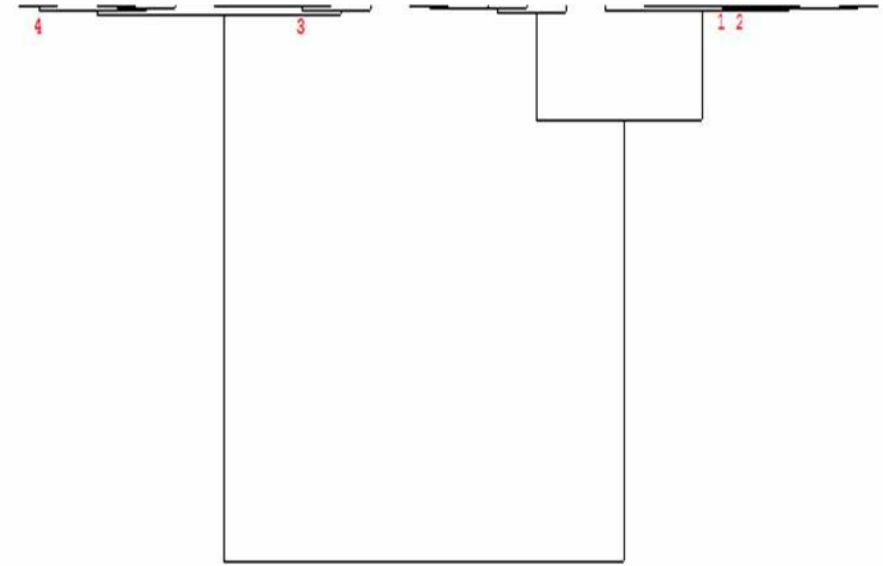
0
50
100
150
200
250
300
350

R_0.05_1.0
R_0.05_2.0
R_0.05_7.0
R_0.05_9.0
R_0.05_8.0
R_0.05_3.0
R_0.05_4.0
R_0.05_5.0
R_0.05_6.0
R_0.1_7.0
R_0.1_1.0
R_0.1_5.0
R_0.1_2.0
R_0.1_6.0
R_0.1_3.0
R_0.1_4.0
C_1.0
C_2.0
C_3.0
C_4.0
C_5.0
C_6.0
C_7.0

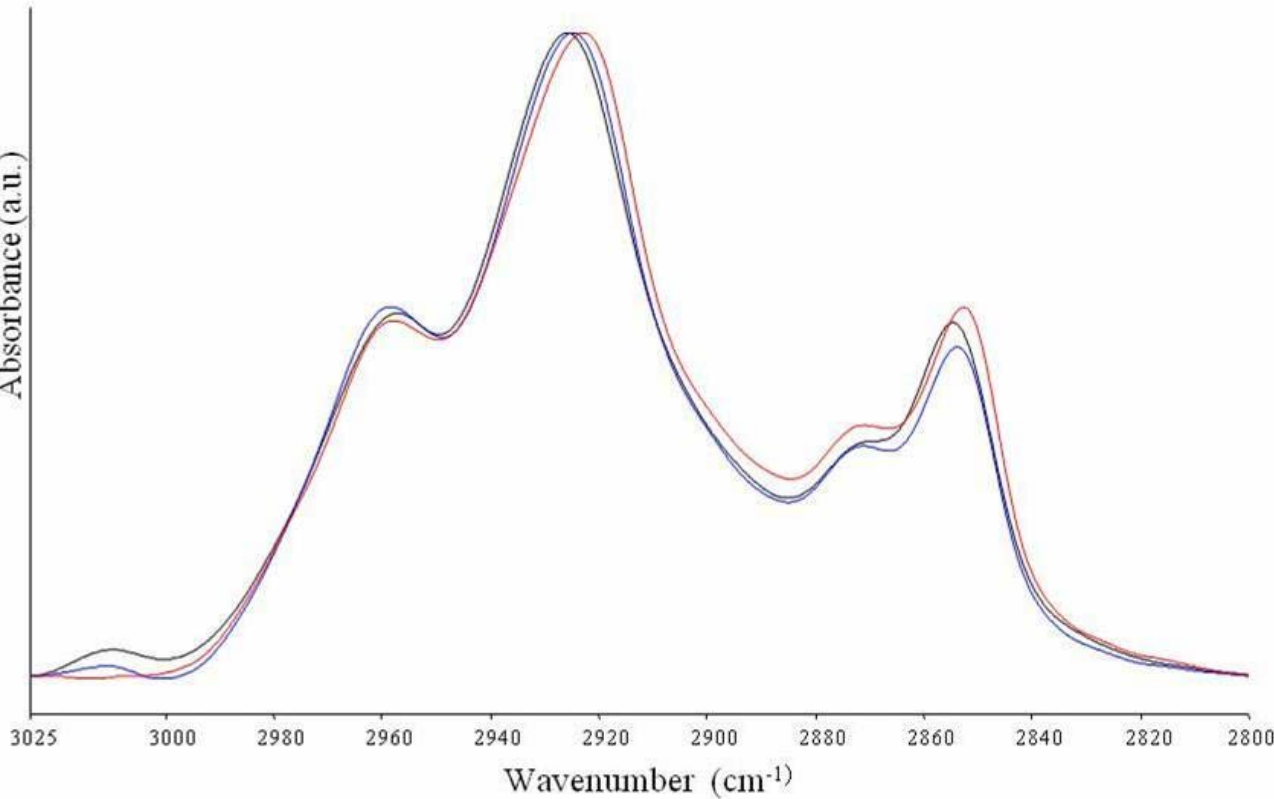
4

3

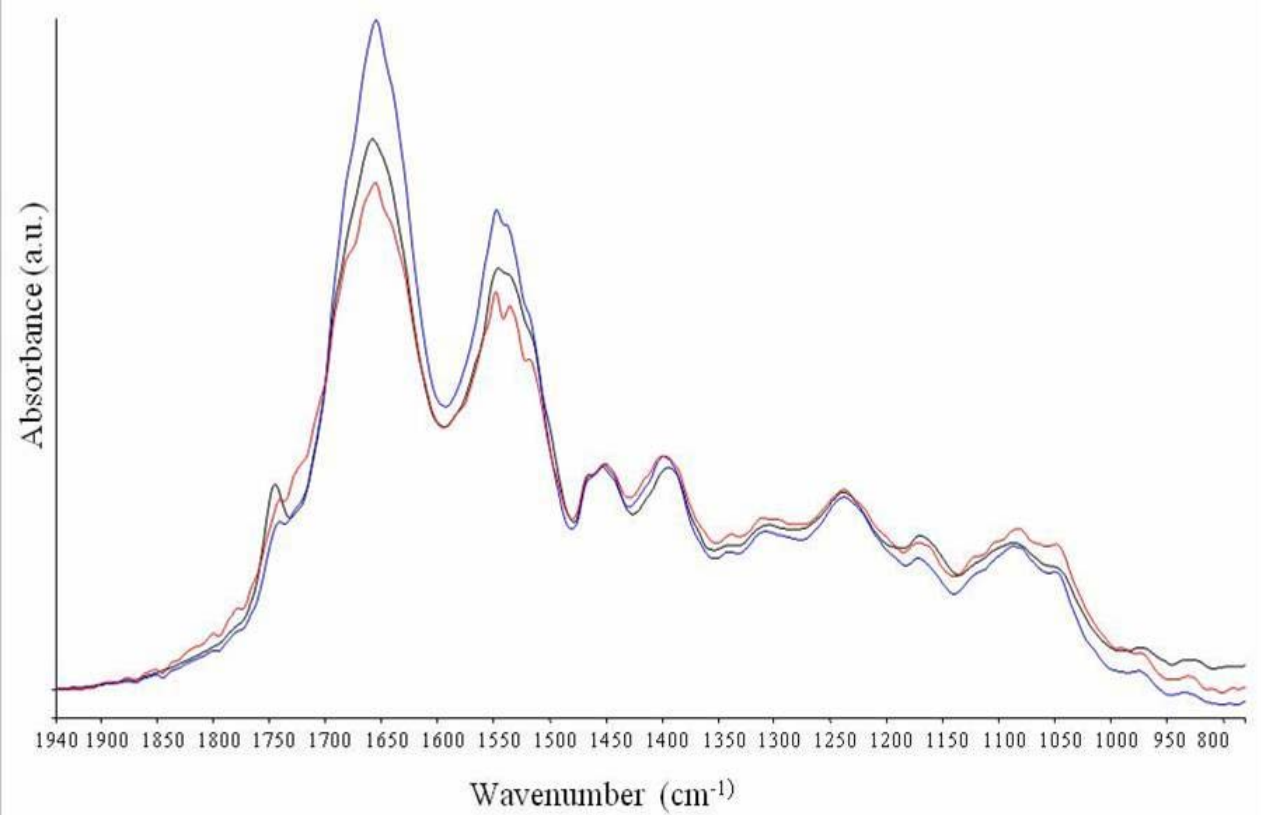
1 2



Absorbance (a.u.)



Wavenumber (cm⁻¹)



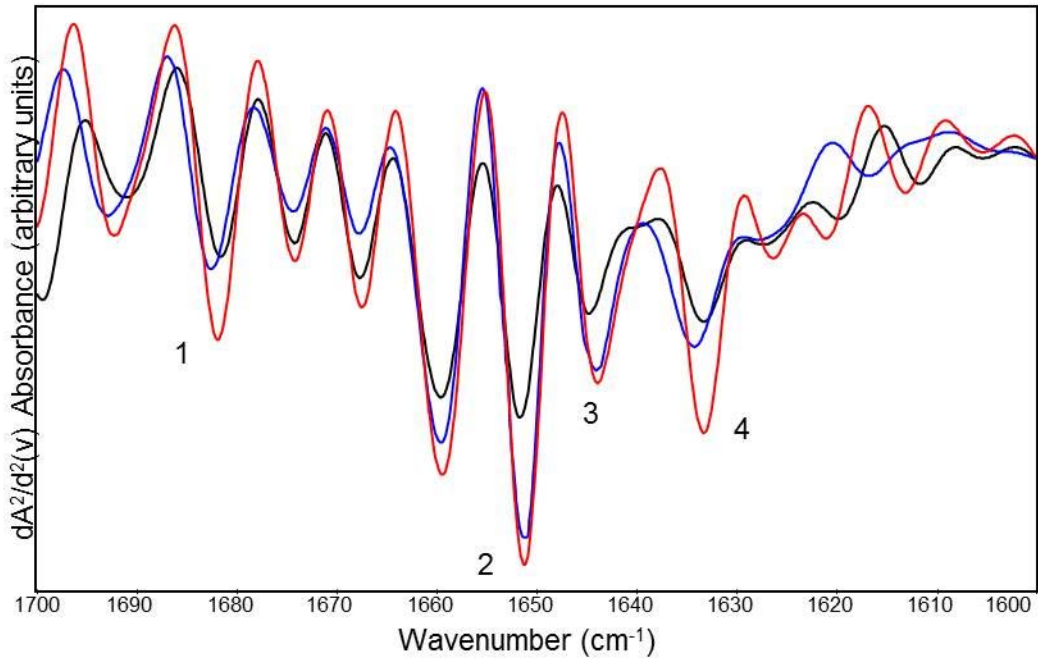


Table 1. General band assignment of heart tissue

Frequency (cm ⁻¹)	Definition of the Spectral Assignments
3012	Olefinic =CH stretching: unsaturated lipids
2925	CH ₂ asymmetric stretching: mainly lipids with little contribution from proteins, carbohydrates and nucleic acids
2852	CH ₂ symmetric stretching: mainly lipid with the little contribution from proteins, carbohydrates and nucleic acids
1750	Saturated ester C=O stretch: phospholipids, cholesterol esters, triglycerides
1645	Amide I (protein C=O stretch): proteins
1547	Amide II (C=N and N-H stretching): proteins
1450	COO ⁻ symmetric stretching: fatty acids
1080	PO ₂ ⁻ symmetric stretching: phospholipids and nucleic acids
976	C ⁺ -N-C stretching: nucleic acids, ribose phosphate main chain vibrations of RNA

Table 2. The frequency, band area and area ratio values of FTIR bands and MDA levels for control, 0.05 mg/kg and 0.1 mg/kg of rolipram for heart tissue. The values are the mean \pm SD for each sample. The degree of significance was denoted as ($p < 0.05^*$).

	Control	0.05 mg/kg	0.1 mg/kg
Frequency			
CH ₂ asym	2924.09 \pm 0.07	2922.14 \pm 0.28*	2921.88 \pm 0.44*
C=O	1753.10 \pm 0.89	1750.62 \pm 1.30*	1750.09 \pm 0.91*
PO ₂ sym	1080.92 \pm 0.58	1077.99 \pm 1.63*	1076.81 \pm 1.12*
Band Areas			
olefinic	1.78 \pm 0.11	1.09 \pm 0.07*	0.34 \pm 0.09**
CH ₂ asym	13.59 \pm 0.76	12.68 \pm 0.14*	11.27 \pm 0.68*
C=O	2.91 \pm 0.03	1.07 \pm 0.08*	0.90 \pm 0.05*
amide I	25.46 \pm 0.78	28.51 \pm 0.49*	20.09 \pm 1.36*
amide II	12.27 \pm 1.43	14.70 \pm 1.41*	10.05 \pm 0.83*
COO ⁻	3.90 \pm 0.06	3.11 \pm 0.17*	3.22 \pm 0.34*
RNA	4.78 \pm 0.67	3.87 \pm 0.39*	3.79 \pm 0.86*
Band Area Ratio Values			
olefinic/lipid	0.08 \pm 0.002	0.05 \pm 0.009*	0.02 \pm 0.004*
CH ₂ /lipid	0.61 \pm 0.009	0.58 \pm 0.007*	0.57 \pm 0.006*
C=O/lipid	0.13 \pm 0.008	0.05 \pm 0.006*	0.04 \pm 0.001*
COO ⁻ /lipid	0.17 \pm 0.002	0.14 \pm 0.002*	0.15 \pm 0.003*
RNA/protein	0.12 \pm 0.007	0.09 \pm 0.008*	0.10 \pm 0.005*
Bandwidth			
CH ₂ asym	8.44 \pm 0.13	8.65 \pm 0.16	8.87 \pm 0.95
TBARs assay			
MDA (nmol/g)	39.44 \pm 2.27	30.05 \pm 1.88*	31.54 \pm 2.90*

Table 3. The changes in value of protein secondary structure estimation by second derivative for control, 0.05 mg/kg and 0.1 mg/kg of rolipram for heart tissue. The values are the mean \pm standart deviation for each sample. The degree of significance was denoted as (p<0.05*).

	Control	0.05 mg/kg rol.	0.1 mg/kg rol.
1-Beta turn	-0.0022 \pm 0.0004	- 0.0019 \pm 0.0002*	- 0.0018 \pm 0.0003*
2-Alpha helix	- 0.0049 \pm 0.0002	- 0.0045 \pm 0.0006*	- 0.0043 \pm 0.0007*
3-Random coil	- 0.0021 \pm 0.0005	- 0.0024 \pm 0.0009*	- 0.0025 \pm 0.0001*
4-Beta sheet	- 0.0036 \pm 0.0007	-0.0026 \pm 0.0004	- 0.0023 \pm 0.0006*